POLITECNICO DI TORINO
Repository ISTITUZIONALE

Reducing CM Conducted EMI in ISOP Flyback Converters Through Balancing Technique

Original
Reducing CM Conducted EMI in ISOP Flyback Converters Through Balancing Technique / Barbaro, A., Choi, S., Raviola, E., Imaoka, J., Fiori, F., Yamamoto, M.. - (2026). (2026 15th International Workshop on the Electromagnetic Compatibility of Integrated Circuits (EMC Compo) Okayama (Jpn) 7-10 December 2026).

Availability:
This version is available at: 11583/3016608 since: 2026-10-13T07:43:57Z

Publisher:
IEEE

Published
DOI:

Terms of use:

This article is made available under terms and conditions as specified in the corresponding bibliographic description in the repository

Publisher copyright
IEEE postprint/Author's Accepted Manuscript

©2026 IEEE. Personal use of this material is permitted. Permission from IEEE must be obtained for all other uses, in any current or future media, including reprinting/republishing this material for advertising or promotional purposes, creating new collecting works, for resale or lists, or reuse of any copyrighted component of this work in other works.

(Article begins on next page)

18 November 2026

Reducing CM Conducted EMI in ISOP Flyback Converters Through Balancing Technique

Alberto Barbaro
Electronics and Telecommunication Department
Politecnico di Torino
Turin, Italy
alberto.barbaro@polito.it

Sihoon Choi
Institute of Materials and Systems for Sustainability
Nagoya University
Nagoya, Japan
choi.sihoon.w4@f.mail.nagoya-u.ac.jp

Erica Raviola
Electronics and Telecommunication Department
Politecnico di Torino
Turin, Italy
erica.raviola@polito.it

Jun Imaoka
Institute of Materials and Systems for Sustainability
Nagoya University
Nagoya, Japan
imaoka.jun.n9@f.mail.nagoya-u.ac.jp

Franco Fiori
Electronics and Telecommunication Department
Politecnico di Torino
Turin, Italy
franco.fiori@polito.it

Masayoshi Yamamoto
Institute of Materials and Systems for Sustainability
Nagoya University
Nagoya, Japan
m.yamamoto@imass.nagoya-u.ac.jp

***Abstract*—In high-voltage to low-voltage isolated power converters for automotive applications, a promising topology is the Input-Series Output-Parallel (ISOP) flyback, allowing to reduce the voltage stress on power transistors. However, Common-mode (CM) conducted Electro-Magnetic Interference (EMI) for such a topology has not yet been thoroughly addressed. This paper investigates the CM EMI reduction at the source by exploiting symmetrical topology combined with balancing technique tailored for ISOP topology. Based on the employed CM equivalent model, the required balancing conditions are derived, leading to a double capacitive compensation which ensures complementary switching waveforms. Simulation results validate the proposed model, allowing a significant CM conducted EMI reduction.**

***Index Terms*—Conducted EMI, flyback ISOP, EMI reduction at the source, symmetric topology, balancing condition.**

I. Introduction

With the increasing demand for efficient and compact High Voltage (HV) to Low Voltage (LV) dc–dc converters, e.g., auxiliary power supplies for traction drives in electric vehicles, isolated topologies derived from the conventional flyback converters have been proposed. Amongst them, the Input-Series Output-Parallel (ISOP) flyback shown in Fig. 1 comprises multiple flyback modules connected in series (parallel) on the HV input (LV output) side [1]. Although its cost is higher, the major advantage compared to a conventional flyback converter is the reduced voltage stress across T_{LS} and T_{HS} transistors, which is approximately halved in the two-cell topology shown in Fig. 1.

By exploiting the ISOP topology, GaN power transistors can be effectively employed in HV to LV conversion, enabling higher switching frequencies and the use of integrated transformers [2], thus further reducing the converter size. However, the use of fast-switching transistors combined with higher switching frequency is expected to increase conducted Electro-Magnetic Interference (EMI) at the converter input, with the drawback of requiring bulky EMI filters. To reduce conducted EMI in power converters, several approaches effective at the source have been proposed in the literature [3]. Besides alternative PWM modulations [4], [5], specific solutions for isolated converters include the adjustment of the transformer winding structure, e.g., shielding or the introduction of dedicated cancellation windings [6], [7]. Other solutions aim at reducing the equivalent parasitic capacitance related to Common-Mode (CM) disturbances [8], thus limiting the CM current injected into the reference ground. A well-known approach is based on symmetric topologies. Originally proposed for boost converters [9], [10], this strategy introduces additional passive or active components to achieve complementary switching nodes, theoretically allowing for a complete CM

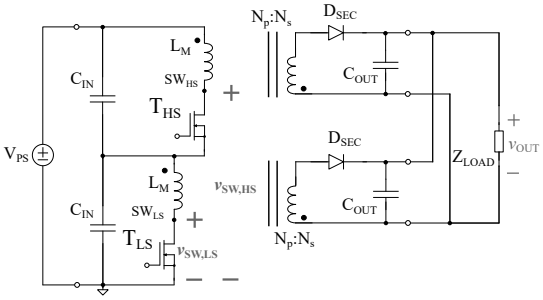


Fig. 1. Traditional ISOP flyback converter.

This publication is part of the project PNRR-NGEU which has received funding from the MUR-DM 117/2023.

cancellation. In order to be effective, symmetric topologies must be combined with balancing techniques, which ensure equal CM current injection from complementary switching nodes [11]. This is typically achieved by including compensation capacitors at specific nodes in order to have equal CM loading. More recently, balancing techniques have also been investigated for conventional [12] and two-switch [13] flyback converters, with promising results.

Although the balancing technique has been widely studied, its application to the ISOP flyback topology remains unexplored. Indeed, the conventional ISOP flyback shown in Fig. 1 is not a symmetric topology. Moreover, since ISOP flyback typically operates in Discontinuous Conduction Mode (DCM), the resonance associated with the magnetizing inductance must be properly addressed not to affect CM EMI cancellation.

This work investigates a symmetric ISOP flyback converter combined with the balancing technique to reduce CM conducted EMI. From the analysis, it results that a double capacitive compensation is required to compensate for CM unbalance and DCM resonance effects at the same time. Simulation results validate the proposed approach.

The paper is organized as follows. Sect. II introduces the symmetric ISOP flyback converter and derives the balancing conditions. Preliminary simulation results are provided in Sect. III to assess the efficacy of the proposed compensation approach. Concluding remarks are in Sect. IV.

II. ISOP CM EQUIVALENT MODEL AND BALANCING CONDITIONS

In the original ISOP flyback configuration shown in Fig. 1, $T_{\rm LS}$ and $T_{\rm HS}$ are driven by the same control signal. This results in the switching-node voltages $v_{\rm SW,HS}(t)$ and $v_{\rm SW,LS}(t)$ to be characterized by simultaneous voltage variations in the same direction, as illustrated in Fig. 4 (a). Therefore, their corresponding CM noise contributions cannot cancel each other out. To obtain a symmetrical configuration, the positions of $T_{\rm HS}$ and the HS primary winding are exchanged, as highlighted in Fig. 2 by a dashed circle. This allows $v_{\rm SW,HS}(t)$ and $v_{\rm SW,LS}(t)$ to exhibit voltage variations in opposite directions, as shown in Fig. 4 (b), enabling cancellation of their CM noise contributions. However, this modification does not ensure exact CM disturbances elimination, as proper balancing conditions must be satisfied.

A. Flyback ISOP CM equivalent model and CM balancing

To investigate the CM conducted EMI of the modified ISOP flyback, hereafter referred to as the symmetrical ISOP flyback, the schematic shown in Fig. 2 is employed. Line Impedance Stabilization Networks (LISNs) have been added and the main parasitics contributing to CM noise have been highlighted by dashed boxes. The coupling between the primary-side switching devices and reference ground is modeled by $C_{\rm SOURCE,g,HS}$ and $C_{\rm DRAIN,g,LS}$, which are associated with the source pad of $T_{\rm HS}$ and the drain pad of $T_{\rm LS}$, respectively. The primary-to-secondary transformer parasitic capacitances are denoted as $C_{\rm ps,HS}$ and $C_{\rm ps,LS}$. Finally, the secondary-side coupling to

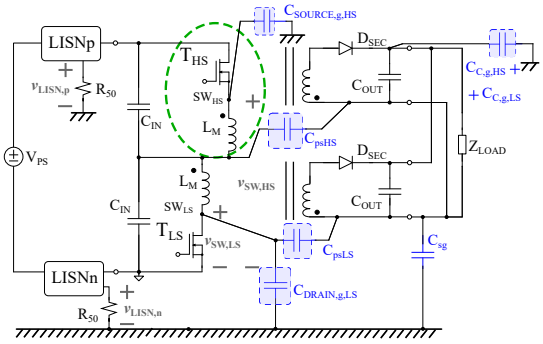


Fig. 2. Schematic of symmetrical ISOP flyback including LISNs for conducted EMI evaluation. The parasitic elements determining CM are encircled in dashed boxes.

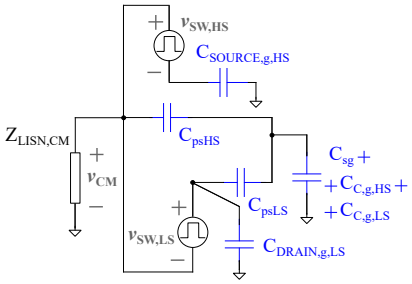


Fig. 3. Simplified equivalent common mode model of symmetrical ISOP flyback.

the reference ground is represented by $C_{\rm C,g,HS}$ and $C_{\rm C,g,LS}$, i.e., those related to the thermal pads of the secondary diodes, and by $C_{\rm sg}$, associated with the secondary ground. From the circuit in Fig. 2, the simplified CM equivalent model shown in Fig. 3 can be derived. As far as the regulated frequency range is concerned, the CM voltage at the LISN side can be approximated in the Laplace domain as

$$V_{\rm CM}(s) = s \cdot Z_{\rm LISN,CM}(s) \cdot C_{\rm n,SW,HS} \cdot V_{\rm SW,HS}(s) + \\ - s \cdot Z_{\rm LISN,CM}(s) \cdot C_{\rm n,SW,LS} \cdot V_{\rm SW,LS}(s), \quad (1)$$

where $C_{\rm n,SW,HS}$ and $C_{\rm n,SW,LS}$ are equivalent capacitances defined as follows

$$C_{\rm n,SW,HS} = C_{\rm SOURCE,g,HS}, \quad (2)$$

$$C_{\rm n,SW,LS} = C_{\rm DRAIN,g,LS} + \\ + \frac{C_{\rm psLS} \cdot (C_{\rm sg} + C_{\rm C,g,HS} + C_{\rm C,g,LS})}{C_{\rm psLS} + C_{\rm psHS} + C_{\rm sg} + C_{\rm C,g,HS} + C_{\rm C,g,LS}}. \quad (3)$$

The overall CM conducted EMI is given by the superposition of HS and LS switching voltages. The minus sign in (1) accounts for the opposite phase of the two noise sources. In what follows, the conditions to ensure the two contributions to be equal are discussed. From (1), assuming that $V_{\rm SW,HS}(s)$ and $V_{\rm SW,LS}(s)$ are equal in magnitude, the first condition to achieve balancing is found by imposing (2) equal to (3). It follows that

$$C_{\rm SOURCE,g,HS} = C_{\rm DRAIN,g,LS} + \\ + \frac{C_{\rm psLS} \cdot (C_{\rm sg} + C_{\rm C,g,HS} + C_{\rm C,g,LS})}{C_{\rm psLS} + C_{\rm psHS} + C_{\rm sg} + C_{\rm C,g,HS} + C_{\rm C,g,LS}}. \quad (4)$$

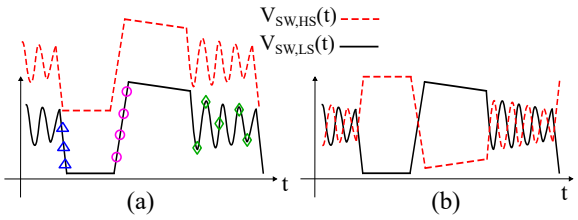


Fig. 4. High-side and low-side switching nodes waveforms for conventional ISOP flyback (a) and symmetrical ISOP flyback (b).

The condition derived in (4) is hereafter referred to as the Common-Mode Balancing (CMB) condition.

B. Noise sources balancing

It is worth noting that (4) only ensures balancing of CM propagation paths under the assumption that $V_{\mathrm{SW,HS}}(s)$ and $V_{\mathrm{SW,LS}}(s)$ are identical. In principle, this may not be true. Assuming DCM operation and neglecting the leakage inductances, the dominant CM contributions arise from three switching-node voltage transitions: turn-on (triangle markers), turn-off (circle markers), and the resonance with magnetizing inductance (diamond markers), as shown in Fig. 4 (a). Both voltage slopes and the trajectories during resonance with the magnetizing inductances are affected by the equivalent capacitances loading the HS and LS switching nodes. Therefore, different values of HS and LS equivalent capacitances may prevent the CM contributions in (1) from perfectly cancelling each other out. With the purpose of evaluating these capacitances, a high-frequency equivalent model can be derived from Fig. 2, following the same approach as for the CM model. The model is omitted for brevity. The expressions of the HS and LS capacitances are reported below

$$C_{\mathrm{eq,HS}} = C_{\mathrm{SOURCE,g,HS}}, \tag{5}$$

$$C_{\mathrm{eq,LS}} = C_{\mathrm{DRAIN,g,LS}} + \\ + C_{\mathrm{psLS}} \oplus (C_{\mathrm{sg}} + C_{\mathrm{C,g,HS}} + C_{\mathrm{C,g,LS}} + C_{\mathrm{psHS}}). \tag{6}$$

where $\oplus$ denotes the parallel combination. The second condition for CM balancing, hereafter referred to as the Noise Sources Balancing (NSB) condition, can be derived by imposing (5) equal to (6). While the CMB condition can be fulfilled by adding a compensation capacitor $C_{\mathrm{comp,1}}$ in parallel with $C_{\mathrm{SOURCE,g,HS}}$, the same approach cannot be used for NSB, since it would modify the CM propagation path and thus violate the CMB condition. For this reason, NSB is achieved by adding a compensation capacitor $C_{\mathrm{comp,2}}$ in parallel with the HS switch, so as to modify the HS switching-node trajectory without altering the CMB condition.

III. Validation Results

The proposed CM balancing analysis has been verified through simulations of both the symmetric ISOP flyback shown in Fig. 2 and the conventional ISOP, using the parameters listed in Table I. In the first step, equivalent capacitances (2) and (3) have been evaluated using the parasitic capacitance values taken from [13] and listed in Table I, yielding $C_{\mathrm{n,SW,HS}} = 10$ pF and $C_{\mathrm{n,SW,LS}} = 20.43$ pF. To satisfy the CMB condition, a compensation capacitor $C_{\mathrm{comp,1}} = 10.43$ pF has been placed in parallel with $C_{\mathrm{SOURCE,g,HS}}$. The resulting switching-node voltages are reported in Fig. 5. Although the CMB is fulfilled, the HS and LS switching-node voltage waveforms are not complementary. More specifically, the resonant transitions associated with the magnetizing inductances are not matched. In the second step, equivalent capacitances (5) and (6) have been evaluated, yielding $C_{\mathrm{eq,HS}} = 20.43$ pF and $C_{\mathrm{eq,LS}} = 55.21$ pF. Hence, a compensation capacitor $C_{\mathrm{comp,2}} = 34.78$ pF has been placed in parallel with the HS switch to satisfy NSB condition. With this additional compensation, complementary switching-node voltage waveforms are obtained, as shown in Fig. 6.

TABLE I
ISOP FLYBACK CONVERTER PARAMETERS.

Parameter	Value	Parameter	Value
V_{PS}; V_{OUT}	400 V; 12 V	P_{OUT}	40 W
Turns ratio	14	L_{M}	536.2 µH
C_{IN}; C_{OUT}	30 µF; 1 mF	f_{SW}	100 kHz
T_{LS}, T_{HS}	GS-065-004-1-L	D_{SEC}	MBR40200PTH
$C_{\mathrm{SOURCE,g,HS}}$	10 pF	C_{sg}; $C_{\mathrm{DRAIN,g,LS}}$	6 pF; 10 pF
$C_{\mathrm{ps,HS}}$, $C_{\mathrm{ps,LS}}$	80 pF	$C_{\mathrm{C,g,HS}}$, $C_{\mathrm{C,g,LS}}$	9 pF

CM spectra have also been evaluated, more precisely, $v_{\mathrm{CM}}(t)$ has been evaluated as $(v_{\mathrm{LISNn}}(t)+v_{\mathrm{LISNp}}(t))/2$ and processed using the Virtual EMI Receiver described in [14]. Resolution bandwidth (RBW) set to 9 kHz for the 150 kHz–30 MHz range and 120 kHz for the 30 MHz–108 MHz range, as prescribed by the standard [15]. Fig. 7 shows the CM EMI spectra of traditional ISOP flyback (black spectrum) compared to symmetrical ISOP flyback in three conditions: without CMB and NSB conditions satisfied (green spectrum), with only CMB condition satisfied (blue spectrum) and, finally, with both conditions satisfied (red spectrum). With only CMB condition satisfied, CM attenuation is limited to the first harmonics, while with both conditions satisfied an attenuation of approximately 50 dB is achieved over a wide frequency range. In practice, the values of the compensation capacitors may deviate from their nominal values due to manufacturing tolerances. To assess the effect of tolerance, in Fig. 8 the CM EMI spectra of traditional ISOP flyback (black spectrum) is compared to the proposed topology with nominal values of compensation capacitors (red spectrum), and with a relative variation of both capacitors of $+10\%$ (green spectrum). With such variation, the achievable attenuation is lowered to approximately 20 dB. The simulated efficiencies for the conventional ISOP flyback and the symmetric ISOP flyback with both CMB and NSB satisfied are 83.5% and 82%, respectively. Thus, the proposed method slightly reduces the efficiency. The additional capacitance may contribute to this reduction by slowing down the switching transitions and increasing switching losses.

IV. Conclusions

A topological modification is proposed for the ISOP flyback converter in order to obtain a symmetrical configuration.

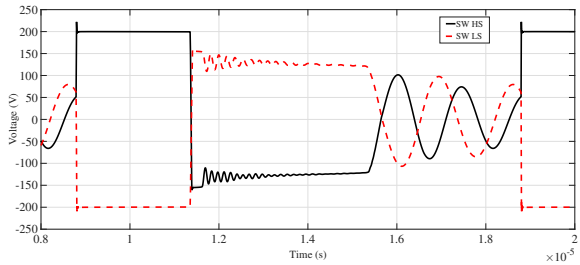


Fig. 5. High side and low side switching node voltages with only CMB condition satisfied

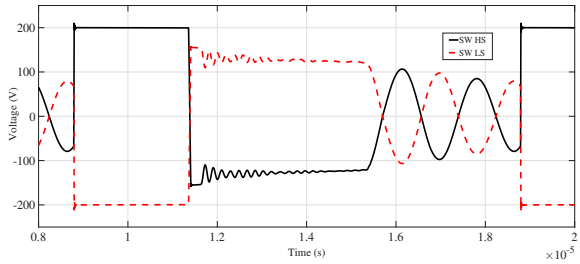


Fig. 6. High side and low side switching node voltages with both CMB and NSB conditions satisfied

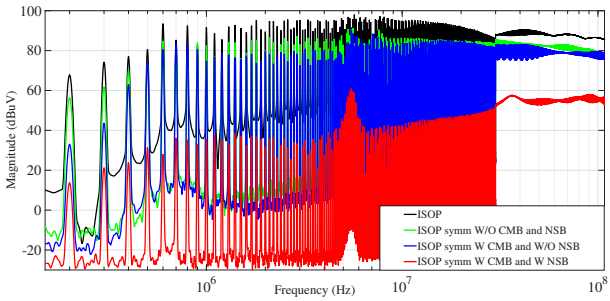


Fig. 7. Comparison of CM EMI frequency spectrum of traditional ISOP flyback, symmetrical ISOP flyback without CMB and NSB satisfied, with only CMB condition satisfied and with both conditions satisfied.

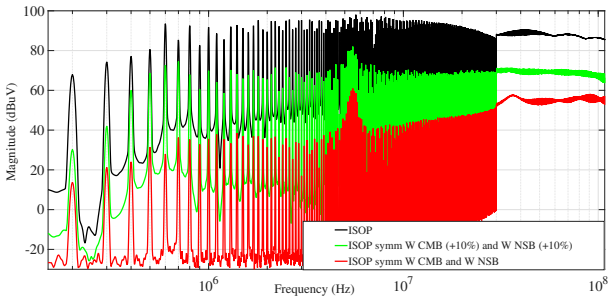


Fig. 8. Comparison of CM EMI frequency spectrum of traditional ISOP flyback, symmetrical ISOP flyback with nominal values of compensation capacitors, and with a relative variation of both capacitors of $+10\%$.

To achieve CM cancellation, two balancing conditions have been identified. Common-mode balancing condition, which balances the CM propagation paths, and the noise sources balancing condition, which ensures HS and LS switching-node voltages to behave as complementary waveforms. Simulation results show that when both CMB and NSB conditions are fulfilled, an attenuation of about 50 dB is obtained. Nevertheless, in a practical implementation nonidealities such as layout parasitics and component tolerances may affect the achievable attenuation. Indeed, it is shown that considering a variation of $+10\%$ of both compensation capacitors may limit the achievable attenuation to 20 dB. Future work will focus on further investigating the proposed approach and, finally, validating the results on a prototype with experimental measurements.

REFERENCES

[1] A. Rodriguez, M. R. Rogina, M. Saeed, D. G. Lamar, M. Arias, M. Lopez, and F. Briz, "Auxiliary power supply based on a modular ISOP flyback configuration with very high input voltage," in *Proc. IEEE Energy Convers. Congr. Expo. (ECCE)*, Sep. 2016, pp. 1–7.

[2] H. Hirasawa, K. R. Dela Cruz Roque, S. Choi, Y. Yonezawa, J. Imaoka, and M. Yamamoto, "Design method of an integrated transformer for a two-phase interleaved flyback pfc rectifier," in *Proc. IEEE Energy Convers. Congr. Expo. (ECCE)*, 2024, pp. 6650–6656.

[3] E. Raviola and F. Fiori, "A software-based control system to reduce conducted cm emi in four-leg three-phase inverters using the delay compensation technique," *IEEE Trans. Circuits Syst. I, Reg. Papers*, vol. 73, no. 6, pp. 4459–4470, 2026.

[4] A. Barbaro, M. Fishta, E. Raviola, and F. Fiori, "A Comparison of Spread Spectrum and Sigma Delta Modulations to Mitigate Conducted EMI in GaN-Based DC-DC Converters," in *Proc. 14th Int. Workshop Electromagn. Compat. Integr. Circuits (EMC Compo)*, Oct. 2024, pp. 1–6.

[5] M. Fishta, E. Raviola, and F. Fiori, "EMI Reduction at the Source in WBG Inverters: A Comparative Study of Spread-Spectrum Modulation and Auxiliary Switching Leg Techniques," *IEEE Trans. Electromagn. Compat.*, vol. 66, no. 5, pp. 1412–1419, Oct. 2024.

[6] L. Xie, "Overview of common-mode noise cancellation techniques for isolated power converters," *Chin. J. Electr. Eng.*, pp. 1–17, 2026.

[7] P. Kong and F. C. Lee, "Transformer structure and its effects on common mode EMI noise in isolated power converters," in *Proc. 25th Annu. IEEE Appl. Power Electron. Conf. Expo. (APEC)*, Feb. 2010, pp. 1424–1429.

[8] Y. Chu and S. Wang, "A Generalized Common-Mode Current Cancelation Approach for Power Converters," *IEEE Trans. Ind. Electron.*, vol. 62, no. 7, pp. 4130–4140, Jul. 2015.

[9] S. Wang, P. Kong, and F. C. Lee, "Common Mode Noise Reduction for Boost Converters Using General Balance Technique," *IEEE Trans. Power Electron.*, vol. 22, no. 4, pp. 1410–1416, Jul. 2007.

[10] T. Nagai, M. Sasaki, J. Imaoka, M. Yamamoto, and A. Nakano, "Balanced Two-phase Interleaved Boost Converter with Integrated Magnetics for Common-Mode Noise Reduction," *IEEJ J. Ind. Appl.*, vol. 12, no. 4, pp. 664–675, 2023.

[11] S. Choi, Y. Yin, J.-W. Shin, J. Imaoka, and M. Yamamoto, "Common-mode noise reduction for bridgeless flyback pfc rectifier with balance technique," in *Proc. IEEE Appl. Power Electron. Conf. Expo. (APEC)*, 2024, pp. 1478–1483.

[12] Y. Bai, X. Yang, D. Zhang, X. Li, W. Chen, and W. Hu, "Conducted EMI Mitigation Schemes in Isolated Switching-Mode Power Supply Without the Need of a Y-Capacitor," *IEEE Trans. Power Electron.*, vol. 32, no. 4, pp. 2687–2703, Apr. 2017.

[13] A. Barbaro, E. Raviola, and F. Fiori, "Reduction of Common Mode Conducted EMI in GaN-Based Two-Switch Flyback Converters Using the Delay Compensation Technique," in *Proc. Int. Symp. Electromagn. Compat. (EMC Europe)*, Sep. 2025, pp. 12–17.

[14] A. Bendicks, T. Dörlemann, C. Krause, and S. Frei, "MATLAB/Octave function to evaluate time-domain signals according to the measurement bandwidth and average/peak detector of EMI test receivers," in *Proc. Conf. Electromagn. Compat. Cologne, Germany*, Jul. 2022, pp. 459–466.

[15] "CISPR 25:2021 - Vehicles, boats and internal combustion engines - Radio disturbance characteristics - Limits and methods of measurement for the protection of on-board receivers," Dec. 2021.